ELECTRONICS AND ELECTRICAL ENGINEERING
ISSN 1392 – 1215 2010. No. 3(99)
ELEKTRONIKA IR ELEKTROTECHNIKA

HIGH FREQUENCY TECHNOLOGY, MICROWAVES
T 191
AUKŠTŲJŲ DAŽNIŲ TECHNOLOGIJA, MIKROBANGOS

Performance Analysis of a Parameterized APES (PAPES) Spectrum Estimation Method for ISAR Applications

G. K. Kalognomos, G. E. Boultadakis, A. V. Karakasiliotis, P. V. Frangos
Division of Information Transmission Systems and Materials Technology, School of Electrical and Computer Engineering, National Technical University of Athens,
9 Iroon Polytechniou Street, Zografou, GR 15773, Athens, Greece, tel.: +30 2107723694; e-mails: georgios.kalognomos@gmail.com, geoboult@ontelecoms.gr, anastasiskarak@yahoo.gr, pfrangos@central.ntua.gr

Introduction

Spectral analysis algorithms are divided in two major categories: *parametric* and *non-parametric*, where the latter apply a narrow band-pass filter to the input signal and the filter output power divided by the filter bandwidth gives a measure of the input signal's spectrum [1]. Many of these methods, like the Capon [2] and the APES [3] estimators, belong to the *matched-filterbank* (MAFI) class [4], which achieve spectral estimation by using adaptive finite impulse response (FIR) filterbanks. Also the C&A algorithm for the estimation of the spectrum of spectral lines was introduced in [5]. Complex spectral estimation methods are important to the Inverse Synthetic Aperture Radar (ISAR) imaging technique which produces 2-D high resolution images of moving targets [6-7]. ISAR research is also related with the development of image reconstruction [8-9], motion compensation and image focusing techniques [10-11]. The use of CAPON and APES for ISAR imaging is discussed in [2], [3] and [12].

In the following section we study a parameterized version of the APES method, referred as Parameterized APES (PAPES) and its efficient implementation. In the third section we propose two algorithms for spectral lines' spectrum estimation. The fourth section includes the results of the simulations performed to prove statements made in this work. Finally, in the last section main conclusions and directions for future related research are provided. The objective is to prove that a PAPES variant outperforms CAPON and APES in terms of frequency resolution, to demonstrate its application to ISAR imaging and to prove that the proposed two algorithms outperform the C&A algorithm in the area of spectral lines' estimation.

Parameterized APES (PAPES) Estimator

First we consider the problem of the spectral estimation of a complex-valued $(N_1 \times N_2)$ discrete-time signal $\{x_{\nu_1,\nu_2}\}$, where $\nu_1 = 0,1,...,N_1-1$ and $\nu_2 = 0,1,...,N_2-1$. Using the filterbank approach [14] and for any frequency pair (ω_1,ω_2) we model x_{ν_1,ν_2} as:

$$x_{\nu_1,\nu_2} = \alpha(\omega_1,\omega_2)\, e^{j(\omega_1\nu_1+\nu_2\omega_2)} + w_{\nu_1,\nu_2}(\omega_1,\omega_2), \quad (1)$$

where $\alpha(\omega_1,\omega_2)$ denotes the complex amplitude of the 2-D sinusoid at (ω_1,ω_2) and $w_{\nu_1,\nu_2}(\omega_1,\omega_2)$ denotes the residual term that includes the noise and interference from the frequency pairs other than (ω_1,ω_2). The problem is reduced now to that of estimating $\alpha(\omega_1,\omega_2)$ from $\{x_{\nu_1,\nu_2}\}$ for all frequency pairs of interest and is solved by passing x_{ν_1,ν_2} through a band pass filter with varying center frequency in order to enhance the sinusoidal components in (1), as well as by obtaining the estimation $\hat{\alpha}(\omega_1,\omega_2)$ from the filtered data [13]. We denote a $(M_1 \times M_2)$ - tap 2-D FIR filter as [13]:

$$\mathbf{h}(\omega_1,\omega_2) = \mathrm{vec}\{\mathbf{H}(\omega_1,\omega_2)\}, \quad (2)$$

where $\mathbf{H}(\omega_1,\omega_2) \in C^{M_1 \times M_2}$ denotes the frequency response of the filter and $\mathrm{vec}\{\ \}$ denotes the operation of stacking the columns of a matrix on top of each other. Let

$$\overline{\mathbf{y}}_{\rho_1,\rho_2} = x(v_1,v_2)\begin{cases} v_1 = \rho_1,\rho_1+1,\ldots,\rho_1+M_1-1, \\ v_2 = \rho_2,\rho_2+1,\ldots,\rho_2+M_2-1, \end{cases} \quad (3)$$

$$\hat{\mathbf{y}}_{\rho_1,\rho_2} = x^*(v_1,v_2)\begin{cases} v_1 = N_1-\rho_1-1,..N_1-\rho_1-M_1, \\ v_2 = N_2-\rho_2-1,..N_2-\rho_2-M_2, \end{cases} \quad (4)$$

be the forward and backward overlapping subvectors of the data vector, where $\rho_1 = 0,1,...,\Lambda_1-1$, $\rho_2 = 0,1,...,\Lambda_2-1$,

$\Lambda_1 = N_1 - M_1 + 1$, $\Lambda_2 = N_2 - M_2 + 1$ and superscript $\{\}^*$ denotes the complex conjugate. Also let

$$\overline{\mathbf{P}}_{\rho_1,\rho_2} = \mathrm{vec}\{\overline{\mathbf{y}}_{\rho_1,\rho_2}\}, \quad (5)$$

$$\hat{\mathbf{P}}_{\rho_1,\rho_2} = \mathrm{vec}\{\hat{\mathbf{y}}_{\rho_1,\rho_2}\}. \quad (6)$$

A solution to the problem of designing $\mathbf{h}(\omega_1,\omega_2)$ is given by the following expression [14]. From this point on we drop the dependence on frequency for notational convenience, unless otherwise needed for clarity reasons:

$$\mathbf{h} = \frac{\mathbf{Q}^{-1}\cdot\mathbf{b}_{M_1,M_2}}{\mathbf{b}^{\mathrm{H}}{}_{M_1,M_2}\cdot\mathbf{Q}^{-1}\cdot\mathbf{b}_{M_1,M_2}}, \quad (7)$$

where

$$\begin{cases}\mathbf{b}_{M_1,M_2}(\omega_1,\omega_2) = \mathbf{b}_{M_2}(\omega_2)\otimes\mathbf{b}_{M_1}(\omega_1),\\ \mathbf{b}_{M_i}(\omega_i) = \left[1 \quad e^{j\omega} \quad \ldots \quad e^{j(M_i-1)\omega}\right]^{\mathrm{T}},\end{cases} \quad (8)$$

Superscript $\{\}^{\mathrm{H}}$ denotes the conjugate transpose, $\{\}^{\mathrm{T}}$ denotes the transpose, operator $\otimes$ denotes the Kronecker matrix product and $\mathbf{Q}(\omega_1,\omega_2)$ represents the covariance matrix of $\mathrm{w}_{v_1,v_2}(\omega_1,\omega_2)$, also known as the noise covariance matrix. The filter in (7) is needed to pass the frequencies undistorted, that is

$$\mathbf{h}^{\mathrm{H}}\cdot\mathbf{b}_{M_1,M_2} = 1. \quad (9)$$

The estimation of $\mathbf{Q}(\omega_1,\omega_2)$ that uses both the forward and the backward data matrices is denoted as $\hat{\mathbf{Q}}_{\text{FB-APES}}(\omega_1,\omega_2)$ and is equal to [13]:

$$\hat{\mathbf{Q}}_{\text{FB-APES}} = \hat{\mathbf{R}} - \frac{1}{\Lambda_1\Lambda_2}\left[\overline{\mathbf{Y}}\cdot\overline{\mathbf{Y}}^{\mathrm{H}} + \hat{\mathbf{Y}}\cdot\hat{\mathbf{Y}}^{\mathrm{H}}\right]. \quad (10)$$

$\overline{\mathbf{Y}}(\omega_1,\omega_2)$ and $\hat{\mathbf{Y}}(\omega_1,\omega_2)$ are the normalized Fourier transforms of the $\overline{\mathbf{P}}_{\rho_1,\rho_2}$, $\hat{\mathbf{P}}_{\rho_1,\rho_2}$ vectors and $\hat{\mathbf{R}}$ is the estimation of the sample covariance matrix $\mathbf{R}$

$$\hat{\mathbf{R}} = \frac{1}{2}\left(\overline{\mathbf{R}} + \hat{\mathbf{R}}\right) = \overline{\mathbf{R}} + \mathbf{J}\overline{\mathbf{R}}^{\mathrm{T}}\mathbf{J}, \quad (11)$$

$$\overline{\mathbf{R}} = \sum_{\rho_2=0}^{\Lambda_2-1}\sum_{\rho_1=0}^{\Lambda_1-1}\overline{\mathbf{P}}_{\rho_1,\rho_2}\cdot\overline{\mathbf{P}}^{\mathrm{H}}{}_{\rho_1,\rho_2}, \quad (12)$$

$$\overline{\mathbf{Y}}(\omega_1,\omega_2) = \sum_{\rho_2=0}^{\Lambda_2-1}\sum_{\rho_1=0}^{\Lambda_1-1}\overline{\mathbf{P}}_{\rho_1,\rho_2}\cdot e^{-j(\rho_1\omega_1+\rho_2\omega_2)}, \quad (13)$$

$$\hat{\mathbf{Y}}(\omega_1,\omega_2) = \sum_{\rho_2=0}^{\Lambda_2-1}\sum_{\rho_1=0}^{\Lambda_1-1}\hat{\mathbf{P}}_{\rho_1,\rho_2}\cdot e^{-j(\rho_1\omega_1+\rho_2\omega_2)}, \quad (14)$$

where $\overline{\mathbf{R}}$ and $\hat{\mathbf{R}}$ are the sample covariance matrices of the $\overline{\mathbf{P}}_{\rho_1,\rho_2}$ and $\hat{\mathbf{P}}_{\rho_1,\rho_2}$ vectors accordingly and $\mathbf{J}$ denotes the exchange matrix whose antidiagonal elements are ones and all the others are zeros.

Forward Backward APES (FB-APES) refers to the APES variant that uses both the forward and the backward data matrices for the estimation of the noise covariance matrix (accordingly F-APES uses only the forward matrices and B-APES only the backward). Similarly, FB-CAPON refers to the CAPON variant that uses both the forward and the backward data matrices for the estimation of the sample covariance matrix (accordingly F-CAPON uses only the forward matrices and B-CAPON only the backward). APES performs better in terms of amplitude estimation [3], but CAPON is less complicated and produces narrower spectral peaks. Both methods outperform FFT in terms of frequency resolution and amplitude estimation [3]. Finally, FB-APES often has better amplitude estimation performance than F-APES [3] and F-CAPON has better frequency resolution than FB-CAPON [5]. The least square (LS) estimate of $\alpha(\omega_1,\omega_2)$ obtained from the filtered data is given by [13]:

$$\hat{\alpha}(\omega_1,\omega_2) = \mathbf{h}^{\mathrm{H}}(\omega_1,\omega_2)\overline{\mathbf{Y}}(\omega_1,\omega_2). \quad (15)$$

Using (10) in (7) we get the expression

$$\mathbf{h}_{\text{FB-APES}} = \frac{\mathbf{Q}^{-1}_{\text{FB-APES}}\cdot\mathbf{b}_{M_1,M_2}}{\mathbf{b}^{\mathrm{H}}{}_{M_1,M_2}\cdot\mathbf{Q}^{-1}_{\text{FB-APES}}\cdot\mathbf{b}_{M_1,M_2}}. \quad (16)$$

Combining (15) and (16) we get the estimation for $a(\omega_1,\omega_2)$ of the FB-APES method as [14]:

$$\hat{\alpha}_{\text{FB-APES}} = \frac{\mathbf{b}^{\mathrm{H}}{}_{M_1,M_2}\cdot\mathbf{Q}^{-1}_{\text{FB-APES}}\cdot\overline{\mathbf{Y}}}{\Lambda_1\Lambda_2\cdot\mathbf{b}^{\mathrm{H}}{}_{M_1,M_2}\cdot\mathbf{Q}^{-1}_{\text{FB-APES}}\cdot\mathbf{b}_{M_1,M_2}}. \quad (17)$$

FB-CAPON method becomes the same with FB-APES when we replace the estimation $\hat{\mathbf{Q}}_{\text{FB-APES}}$ with $\hat{\mathbf{R}}$.

A parameterization of the estimation of the noise covariance matrix with one parameter was originally proposed in [14] as a topic for future research. A first study of such a parameterization with one parameter was introduced in [15] for the 1-D case. Now we make a different intuitive choice for the estimator of the noise covariance matrix, which we denote as $\hat{\mathbf{Q}}_{\text{PAPES}}(\omega_1,\omega_2)$, by introducing two parameters (κ_1,κ_2) in (10), that is

$$\hat{\mathbf{Q}}_{\text{PAPES}} = \hat{\mathbf{R}} - \frac{1}{\Lambda_1\Lambda_2}\left[\kappa_1\overline{\mathbf{Y}}\cdot\overline{\mathbf{Y}}^{\mathrm{H}} + \kappa_2\hat{\mathbf{Y}}\cdot\hat{\mathbf{Y}}^{\mathrm{H}}\right]. \quad (18)$$

This parameterization, which produces the proposed PAPES method, is actually implemented by weighting the contribution of the normalized Fourier transforms $\overline{\mathbf{Y}}(\omega_1,\omega_2)$, $\hat{\mathbf{Y}}(\omega_1,\omega_2)$ of the $\overline{\mathbf{P}}_{\rho_1,\rho_2}$, $\hat{\mathbf{P}}_{\rho_1,\rho_2}$ vectors to estimate the noise covariance matrix. Using (18) in (7) and combining the result with (15) we get the estimation for $\alpha(\omega_1,\omega_2)$ using the 2-D PAPES method as [13]:

$$\hat{\alpha}_{\text{PAPES}} = \frac{\mathbf{b}^{\mathrm{H}}{}_{M_1,M_2}\cdot\mathbf{Q}^{-1}_{\text{PAPES}}\cdot\overline{\mathbf{Y}}}{\Lambda_1\Lambda_2\cdot\mathbf{b}^{\mathrm{H}}{}_{M_1,M_2}\cdot\mathbf{Q}^{-1}_{\text{PAPES}}\cdot\mathbf{b}_{M_1,M_2}}. \quad (19)$$

It is directly verified that PAPES reduces to FB-CAPON when the parameters are equal to 0 and to FB-APES when they are equal to 1. Additionally we denote as Backward PAPES (B-PAPES) the PAPES variant for $(\kappa_1,\kappa_2)=(0,1)$ and as Forward PAPES (F-PAPES) the PAPES variant for $(\kappa_1,\kappa_2)=(1,0)$ [see (18)].

Efficient implementations of the CAPON and APES methods were introduced in [16] and [17] to reduce the computation time needed for their application. Using (18) and (19) and applying the Matrix Inversion lemma [1] appropriately, we obtain the following expression:

$$\hat{\alpha}_{\mathrm{PAPES}}=\frac{\mathbf{b}^{\mathrm{H}}{}_{M_1,M_2}\cdot\overline{\mathbf{Q}}^{-1}_{\mathrm{PAPES}}\cdot\overline{\mathbf{Y}}}{\left(\Lambda_1\Lambda_2-\kappa_1\overline{\mathbf{Y}}^{\mathrm{H}}\overline{\mathbf{Q}}^{-1}_{\mathrm{PAPES}}\cdot\overline{\mathbf{Y}}\right)\times}$$

$$\times\mathbf{b}^{\mathrm{H}}{}_{M_1,M_2}\cdot\overline{\mathbf{Q}}^{-1}_{\mathrm{PAPES}}\cdot\mathbf{b}_{M_1,M_2}+$$

$$+\kappa_1\left|\mathbf{b}^{\mathrm{H}}{}_{M_1,M_2}\cdot\overline{\mathbf{Q}}^{-1}_{\mathrm{PAPES}}\cdot\overline{\mathbf{Y}}\right|^2}, \qquad (20)$$

where

$$\overline{\mathbf{Q}}^{-1}{}_{\mathrm{PAPES}}=\hat{\mathbf{R}}^{-1}+\kappa_2\hat{\mathbf{R}}^{-1}\frac{\hat{\mathbf{Y}}\hat{\mathbf{Y}}^{\mathrm{H}}\hat{\mathbf{R}}^{-1}}{\Lambda_1\Lambda_2-\kappa_2\hat{\mathbf{Y}}^{\mathrm{H}}\hat{\mathbf{R}}^{-1}\hat{\mathbf{Y}}}. \qquad (21)$$

It is directly verified that modifying the methodology of [16] with the appropriate use of (20) and (21) results to an efficiently implementation of the PAPES method.

Combining the PAPES and APES Methods for the Complex Estimation of Spectral Lines

The combination of the CAPON and the APES methods, by the means of the C&A algorithm, was introduced in [5] for the purposes of the complex estimation of spectral lines. C&A estimates first the spectral peak locations using F-CAPON and then estimates the amplitude and phase at those peak locations using FB-APES. As proven in [5], C&A outperforms CAPON and APES in the problem of the estimation of spectral lines, since F-CAPON has better frequency resolution than any other CAPON or APES variant. Now we propose two algorithms for the complex estimation of spectral lines.

The first algorithm (CPAPES-1) is proposed for the estimation of the amplitude of spectral lines and is comprised of two steps: (a) Estimation of the spectral peak locations using B-PAPES, which is expected to perform better than F-CAPON in terms of frequency resolution and (b) Estimation of the spectral lines' amplitude at the locations obtained in step (a) using FB-APES. The second algorithm (CPAPES-2) is proposed for the estimation of the phase of spectral lines and is comprised of two steps: (a) Estimation of the spectral peak locations using F-PAPES and (b) Estimation of the phase of the spectral lines at the locations obtained in step (a) using F-PAPES.

Numerical Examples

All simulations mentioned in this section were performed using a PC with a Q6600 CPU and 4 Gb DDR2 RAM. The results of the simulations concerning 1-D data were obtained for 500 independent noise realizations (zero-mean complex white Gaussian noise).

First we used a 1-D synthetic data sequence of N=128 samples. The true spectrum of the simulated sinusoidal signal consists of two spectral lines with complex amplitude $\sqrt{0.5}+\sqrt{0.5}\mathrm{i}$ and corresponding phase $\pi/4$. The first line is located at the normalized frequency 0.0781, while the location of the second varies from 0.0781 to 0.0914 with a step of 0.05/N. The complex spectrum was evaluated at 5120 equally spaced frequency points.

The simulations that gave the results shown in Fig. 1 were performed to demonstrate the frequency resolution performance of the FB-CAPON, FB-APES, B-PAPES and F-CAPON methods, by studying the missed peaks ratio vs. the frequency separation of the two spectral lines. The simulations were performed by the use of a commonly used rule, which quantifies the capability of a method to resolve two sinusoidal signals [18]. As we can see, the performance of B-PAPES in terms of frequency resolution appears to be better than that of the other methods, even than that of the F-CAPON. Additional simulations (not shown here) gave similar results for other M/SNR values (32/0, 64/0, 64/20) and showed that for SNR<0 dB, the frequency resolution performance of B-PAPES and F-CAPON appears to converge until it is practically the same (when SNR<-10 dB). Further simulations concerning all the other PAPES variants for which $\kappa_1,\kappa_2\in[0,1]$ didn't give promising results in terms of frequency resolution.

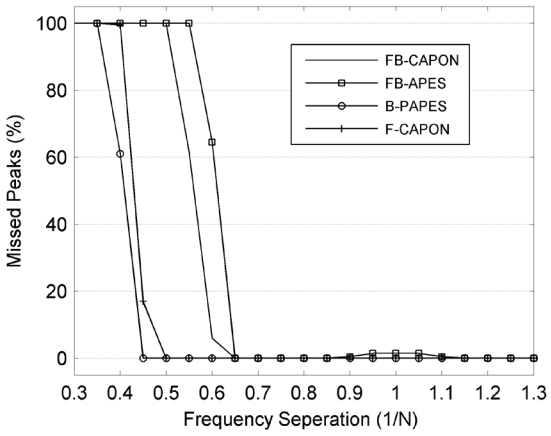

Fig. 1. Frequency resolution for filter length M=32 and SNR=20 dB in the case of two spectral lines

Next we used another 1-D synthetic data sequence of N=128 samples. The true spectrum of the simulated sinusoidal signal consists of 5 spectral lines with complex amplitude $\sqrt{0.5}+\sqrt{0.5}\mathrm{i}$ and corresponding phase $\pi/4$. The spectral lines are located at the normalized frequencies 0.0781, 0.3125, 0.3438, 0.3906 and 0.3945. The frequency separation is $4/N$ between the second and the third line and $0.5/N$ between the fourth and the fifth. Complex spectrum was evaluated at 1024 equally spaced frequency points.

The simulations that gave the results shown in Figure 2 were performed to demonstrate the amplitude estimation

performance of the F-CAPON and B-PAPES methods, by studying the amplitude bias estimation error of the second and the fourth spectral line vs. the filter length M. As we can see from these results, the amplitude estimation performance of B-PAPES appears to be better than that of F-CAPON, both in small and large frequency separation scenarios. Our simulations have also confirmed that the two methods have practically the same phase estimation performance in all frequency separation cases. These conclusions are also confirmed for SNR=0 dB and when the estimation error is studied vs. the SNR. Further simulations concerning all the PAPES variants for which $\kappa_1, \kappa_2 \in [0,1]$, showed that they give no promising results in terms of amplitude estimation performance when compared to the APES method.

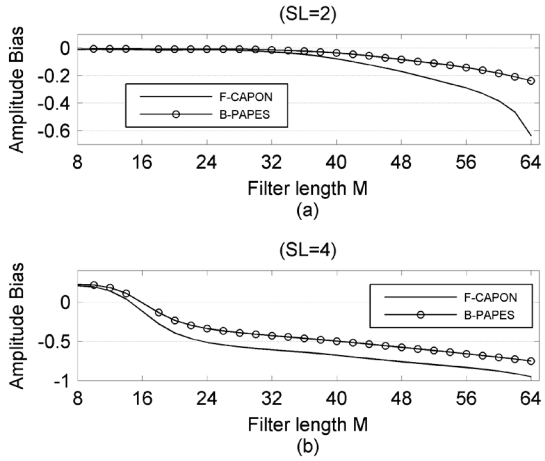

Fig. 2. Amplitude Bias vs. filter length M in the case of five spectral lines for SNR=20 dB and for (a) SL=2 and (b) SL=4, where SL denotes the number of the spectral line

Fig. 3 shows the results of the simulations performed to demonstrate the amplitude, phase and frequency estimation performance of the CAPES, C&A, CPAPES-1 and CPAPES-2 algorithms, by studying the amplitude/phase/frequency bias estimation errors of the fourth spectral line vs. the filter length M. The difference between C&A and CAPES is that the latter uses FB-APES to estimate the peak's location. The frequency bias, measured in frequency points, is the difference between the true frequency of the fourth spectral line and the frequency where each method produces the fourth spectral peak. The latter is calculated by finding the local amplitude max inside an appropriate window of frequency points.

As we can see from these results, CPAPES-1 appears to outperform the other algorithms in terms of amplitude and frequency estimation performance, when the frequency separation of the spectral lines is small ($0.5/N$). Further simulations (not presented here) gave similar results for SNR=0 dB and showed that CPAPES-2 appears to outperform the other algorithms in terms of phase estimation performance for small ($0.5/N$) frequency separation scenarios. Finally, it is has been confirmed by our simulations that the amplitude/phase/frequency estimation performance of all four algorithms is practically the same when the frequency separation of the spectral lines is large, as it is the case for the lower three spectral lines. These conclusions are also confirmed when the estimation errors are studied vs. the SNR.

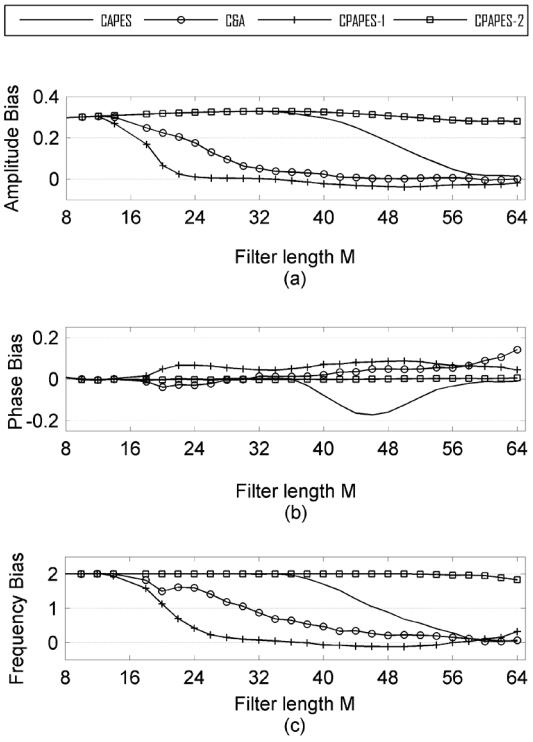

Fig. 3. Amplitude/Phase/Frequency Bias vs. filter length M for the fourth spectral line, out of totally five and for SNR=20 dB

Fig. 4 shows the results of the simulations performed to evaluate the capability of the CAPES, C&A and CPAPES-1 algorithms to resolve the fourth and fifth spectral line (separated in frequency by $0.5/N$), by studying the failure to resolve the two lines ratio vs. SNR and the filter length M (not shown here). It is clear that the CPAPES-1 algorithm appears to outperform the other two algorithms in all cases.

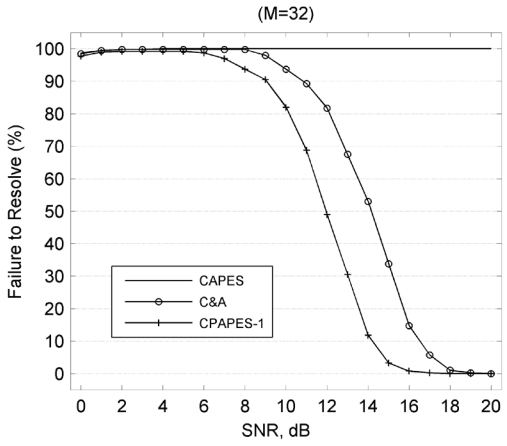

Fig. 4. Failure to Resolve (%) vs. SNR for filter length M=32 and for the upper two spectral lines, out of totally five, with frequency separation $0.5/N$

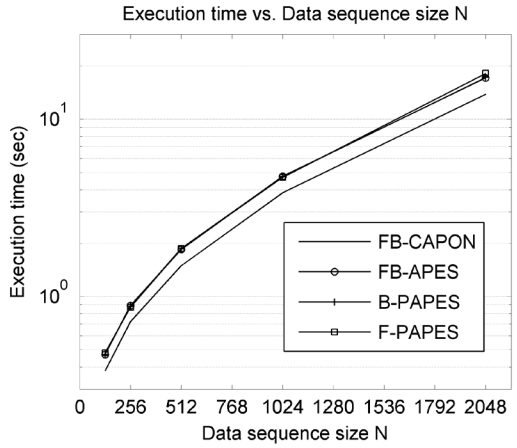

Fig. 5. Execution time for filter length *M*=*N*/2 and SNR=14 dB in the case of random 1-D data sequences

Fig. 5 shows the results of the simulations performed to study the execution time needed to efficiently implement the FB-CAPON, FB-APES, B-PAPES and F-PAPES methods, using the method proposed in [16] for the first two and the method proposed in the second section for the last two. We used random 1-D data sequences of varying *N* and we kept *M* equal to *N*/2. The spectrum was evaluated at 4096 equally spaced frequency points.

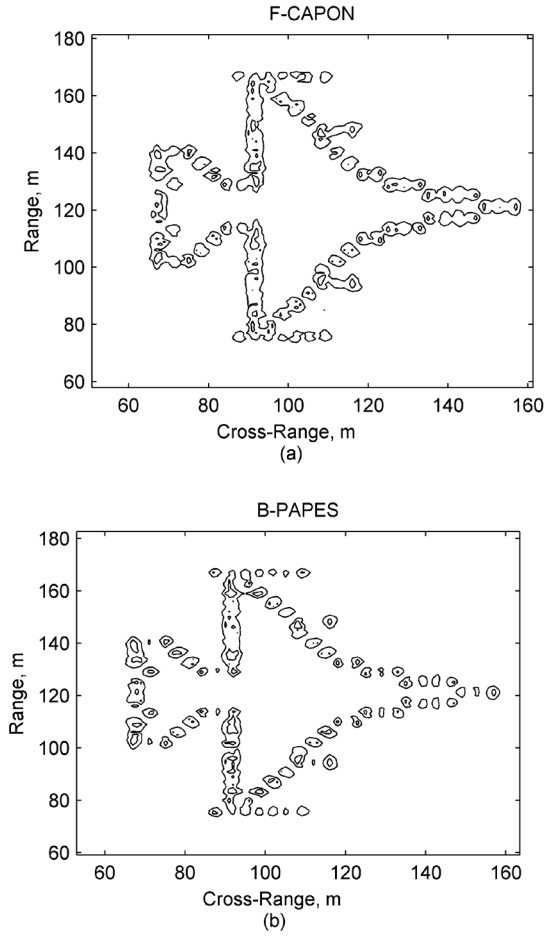

Fig. 6. ISAR images of a simulated F-16 aircraft for filter length *M*=*N*/2 and SNR=8 dB, produced with the (a) F-CAPON and (b) B-PAPES methods

The execution time was essentially the same for the four methods and about 28 times smaller (for *N*=128) than the time measured using the methodology of [4] and [13]. The latter and the fact that FB-CAPON's execution time was about 1.6 times smaller compared to that of the other methods agree with the findings of [16]. Based on these results and on the complexity comparison made in [17] between the methods of [16] and [17], we can safely assume that using the method of [17] to efficiently implement PAPES will produce even better results.

Finally, we consider the ISAR imaging of a simulated F-16 aircraft, which model consists of 257 points scatterers arranged in a 30x30 grid. The image reconstruction was performed for filter lengths $M_1 = N_1/2 = 62$ (cross-range) and $M_2 = N_2/2 = 56$ (range), after polar reformatting. The complex spectrum was evaluated for $2N_1 = 248$ and $2N_2 = 224$ frequency points. The SNR is 8 dB and a stepped-frequency waveform with a 10 GHz carrier frequency and a 800 MHz bandwidth is used. PRF is 18 kHz and integration time is 1.48 sec. The aircraft is rotating at 8 deg/sec, its range is 4000 m, range resolution is 0.1875 m and cross-range resolution is 0.0726 m [19].

Fig. 6 shows the reconstructed ISAR images (2 level contour plots) produced using the F-CAPON and B-PAPES methods. It can be easily verified that more scatterers are resolved in the image produced by B-PAPES than in the one produced by the other method.

Conclusions and Future Research Directions

In this paper we introduced the PAPES method, we demonstrated its application to ISAR imaging and we proposed two new algorithms for spectral lines' spectrum estimation. By means of extensive simulations, we validated the following main conclusions:

a. B-PAPES method appears to outperform all the CAPON and APES variants (even F-CAPON) in terms of frequency resolution, to outperform F-CAPON in terms of amplitude estimation performance in all SNR and frequency separation scenarios and to have practically the same phase estimation performance with F-CAPON. This makes B-PAPES a very suitable candidate for complex spectrum estimation applications like ISAR imaging, where the frequency resolution is of the highest importance, even for low SNR scenarios.

b. The CPAPES-1 algorithm appears to outperform the C&A algorithm in terms of spectral lines' amplitude/phase/frequency estimation performance for small frequency separation scenarios and to exhibit similar performance for large frequency separation scenarios. This makes CPAPES-1 a very suitable candidate for applications concerning complex estimation of spectral lines in all cases, as compared to the C&A algorithm.

c. The CPAPES-2 algorithm appears to outperform CPAPES-1 and C&A in terms of spectral lines' phase estimation performance for small frequency separation scenarios and to exhibit similar performance for large frequency separation scenarios. This makes CPAPES-2 a very suitable candidate for spectral lines' spectrum estimation applications, where the phase estimation performance is of the biggest importance.

Research study is in progress to further investigate the relation of the proposed APES's parameterization to the performance aspects of the spectrum estimation problem and to adapt the efficient method proposed in [18] to PAPES. Finally, we will investigate the use of CPAPES for target classification.

References

1. **Stoica P., Moses R.** Spectral analysis of signals. – Pearson/Prentice Hall. – 2005.
2. **Capon J.** High-resolution frequency-wavenumber spectrum analysis // Proceedings of IEEE. – 1969. – Vol. 57, No. 8. – P. 1408–1418.
3. **Li J., Stoica P.** An adaptive filtering approach to spectral estimation and SAR imaging // IEEE Transactions on Signal Processing. – 1996. – Vol. 44, No. 6. – P. 1469–1484.
4. **Stoica P., Jakobsson A., Li J.** Matched-filter bank interpretation of some spectral estimators // Signal Processing. – 1998. – Vol. 66, No. 1. – P. 45–59.
5. **Jakobsson A., Stoica P.** Combining Capon and APES for estimation of spectral lines // Circ. Systems and Signal Processing. – 2000. – Vol. 19, No. 2. – P. 159–168.
6. **Rihaczek A. W., Hershkowitz S. J.** Theory and practice of radar target identification. – Artech House. – 2000.
7. **Chen C. C., Andrews H. C.** Target-motion-induced radar imaging // IEEE Trans. Aerosp. Electron. Systems. – 1980. – Vol. 16, No. 1. – P. 2–14.
8. **Hua Y., Baqai F., Zhu Y., Heilbronn D.** Imaging of point scatterers from step-frequency ISAR data // IEEE Trans. Aerosp. Electron. Systems. – 1993. – Vol. 19, No. 1. – P. 195–205.
9. **Karakasiliotis A. V., Lazarov A. D., Frangos P. V., Boultadakis G., Kalognomos G. K.** Two-dimensional ISAR model and image reconstruction with stepped frequency-modulated signal // IET Signal Processing. – 2008. – Vol. 2, No. 3. – P. 277–290.
10. **Qian S., Chen D.** Joint time-frequency analysis: methods and applications. – Prentice-Hall Inc. – 1996.
11. **Boultadakis G. E., Kalognomos G. K., Karakasiliotis A. V., Frangos P. V., Stergioulas L. K.** A Comparative Study of Bilinear Time-Frequency Transforms of ISAR Signals for Air Target Imaging // Electronics and Electrical Engineering. – Kaunas: Technologija, 2009. – No. 4(92). – P. 87–92.
12. **Liu Z.-S., Wu R., Li J.** Complex ISAR imaging of maneuvering targets via the CAPON estimator // IEEE Transactions on Signal Processing. – 1999. – Vol. 47, No. 5. – P. 1262–1271.
13. **Li H., Li J., Stoica P.** Performance analysis of forward-backward matched-filterbank spectral estimators // IEEE Transactions on Signal Processing. – 1998. – Vol. 46, No. 7. – P. 1954–1966.
14. **Jakobsson A.** Model-Based and Matched-Filterbank Signal Analysis / Ph.D. Thesis. – Uppsala University, Sweden. – 2000.
15. **Kalognomos G., Frangos P.** Combining capon and APES noise covariance estimates for spectral estimation for ISAR applications // Proceeding of RAST 2005. – Istanbul, Turkey. – 2005. – P. 694–698.
16. **Liu Z., Li H., Li J.** Efficient implementation of Capon and APES for spectral estimation // IEEE Trans. Aerosp. Electron. Systems. – 1998. – Vol. 34, No. 4. – P. 1314–1319.
17. **Larsson E., Stoica P.** Fast implementation of two-dimensional Capon and APES spectral estimators // Multidimensional Systems and Signal Processing. – 2002. – Vol. 13, No. 1. – P. 33–53.
18. **Zhang Q.** A statistical resolution theory of the AR method of spectral analysis // IEEE Transactions on Signal Processing. – 1998. – Vol. 46, No. 10. – P. 2757–2766.
19. **Wehner D. R.** High resolution radar (2^{nd} edn.). – Artech House. – 1995.

Received 2009 11 20

G. K. Kalognomos, G. E. Boultadakis, A. V. Karakasiliotis, P. V. Frangos. Performance Analysis of a Parameterized APES (PAPES) Spectrum Estimation Method for ISAR Applications // Electronics and Electrical Engineering. – Kaunas: Technologija, 2010. – No. 3(99). – P. 43–48.

A parameterized version of the non-parametric APES (Amplitude and Phase Estimation of a Sinusoid) spectrum estimation method, its application to Inverse Synthetic Aperture Radar (ISAR) imaging is studied and two algorithms for the estimation of complex spectral lines are proposed. The proposed method, referred as Parameterized APES (PAPES), is produced by a parameterization of the estimation of the noise covariance matrix using two parameters. We prove that the performance of the PAPES variant referred as Backward PAPES (B-PAPES) method exceeds that of CAPON and APES in terms of frequency resolution. We also prove that the proposed two algorithms outperform the existing C&A (Capon & APES) algorithm in the area of spectral lines estimation. Ill. 6, bibl. 19 (in English; summaries in English, Russian and Lithuanian).

Г. К. Калогномос, Г. Е. Боултадакис, А. В. Каракасилиотис, П. В. Франгос. Анализ производительности параметризованного метода оценки спектра APES (PAPES) для использования в ISAR // Электроника и электротехника. – Каунас: Технология, 2010. – № 3(99). – С. 43–48.

Предлагается параметризованная версия метода оценки спектра APES, изучено его применение в ISAR изображения, а также два алгоритма для оценки сложных спектральных линий. Предлагаемый метод (PAPES) получен путем параметризации оценки ковариационной матрицы шумов с помощью двух параметров. Доказано, что эффективность отдельного варианта метода PAPES (B-PAPES) превышает эффективность CAPON и APES с точки зрения резолюции частоты. Также доказано, что предлагаемые алгоритмы превосходят существующие C & A (Capon & Apes) алгоритмы в области оценивания спектральных линий. Ил. 6, библ. 19 (на английском языке; рефераты на английском, русском и литовском яз.).

G. K. Kalognomos, G. E. Boultadakis, A. V. Karakasiliotis, P. V. Frangos. Parametrizuoto APES (PAPES) spektro įvertinimo metodo taikymo ISAR srityje našumo analizė // Elektronika ir elektrotechnika. – Kaunas: Technologija, 2010. – Nr. 3(99). – P. 43–48.

Pasiūlyta parametrizuota APES (angl. Amplitude and Phase Estimation of a Sinusoid) spektro įvertinimo metodo versija, aptariamas jos taikymas ISAR (angl. Inverse Synthetic Aperture Radar) vaizdams apdoroti ir dviejų algoritmų panaudojimas kompleksinėms spektro linijoms įvertinti. Siūlomas metodas (PAPES) sukurtas parametrizuojant triukšmo kovariacijos matricos įvertį naudojant du parametrus. Įrodyta, jog PAPES modifikacijos B-PAPES našumas viršija CAPON ir APES našumą, atsižvelgiant į dažnio skiriamąją gebą. Taip pat įrodyta, jog naudojant du pasiūlytuosius algoritmus spektrinėms linijoms įvertinti gaunamas geresnis efektas negu naudojant C&A (Capon & APES) algoritmus. Il. 6, bibl. 19 (anglų kalba; santraukos anglų, rusų ir lietuvių k.).